

N O T I C E

THIS DOCUMENT HAS BEEN REPRODUCED FROM
MICROFICHE. ALTHOUGH IT IS RECOGNIZED THAT
CERTAIN PORTIONS ARE ILLEGIBLE, IT IS BEING RELEASED
IN THE INTEREST OF MAKING AVAILABLE AS MUCH
INFORMATION AS POSSIBLE

ERC41054.36FR

ERC41054.36FR

Copy No. **16**

HIGH PURITY LOW DISLOCATION GaAs SINGLE CRYSTALS

FINAL REPORT FOR THE PERIOD
February 25, 1980 through February 24, 1981

CONTRACT NO. NAS3-22224

Prepared for

NASA-Lewis Research Center
Cleveland, OH 44135

R.T. Chen
Principal Investigator

JANUARY 1982



*Approved for public release; distribution unlimited



Rockwell International

Microelectronics Research
and Development Center

CR- 55593

NR2-23030

Unclass
09570

(NASA-CR-165593) HIGH PURITY LOW
DISLOCATION GaAs SINGLE CRYSTALS Final
Report, 25 Feb. 1980 - 24 Feb. 1981
(Rockwell International Corp., Thousand
Oaks) 46 p HC A03/MF A01 CSCI 20B G3/76

ERC41054.36FR

ERC41054.36FR

Copy No. 16

HIGH PURITY LOW DISLOCATION GaAs SINGLE CRYSTALS

FINAL REPORT FOR THE PERIOD
February 25, 1980 through February 24, 1981

CONTRACT NO. NAS3-22224

Prepared for

NASA-Lewis Research Center
Cleveland, OH 44135

R.T. Chen
Principal Investigator

JANUARY 1982



*Approved for public release; distribution unlimited



Rockwell International

Microelectronics Research
and Development Center

CR-1 55593

N82-23030

Unclas
C9570

(NASA-CR-105593) HIGH PURITY LOW
DISLOCATION GaAs SINGLE CRYSTALS Final
Report, 25 Feb. 1980 - 24 Feb. 1981
(Rockwell International Corp., Thousand
Oaks) 46 p HC A03/EF A01 CSCI 20B G3/7b

| | | | | | |
|---|--|--|--|---|--|
| 1. Report No CR 165593 | | 2. Government Accession No. | | 3. Recipient's Catalog No. | |
| 4. Title and Subtitle High Purity, Low Dislocation GaAs Single Crystals | | | | 5. Report Date January 1982 | |
| | | | | 6. Performing Organization Code | |
| 7. Author(s) R.T. Chen, D.E. Holmes, C.G. Kirkpatrick | | | | 8. Performing Organization Report No ERC41054.36FR | |
| 9. Performing Organization Name and Address Rockwell International Microelectronics Research & Development Center 1049 Camino Dos Rios Thousand Oaks, CA 91360 | | | | 10. Work Unit No. | |
| | | | | 11. Contract or Grant No. NAS3-22224 | |
| 12. Sponsoring Agency Name and Address Lewis Research Center Cleveland, Ohio 44135 | | | | 13. Type of Report and Period Covered FINAL - 3/2/81 2/25/80 - 2/24/81 | |
| | | | | 14. Sponsoring Agency Code 4231 | |
| 15. Supplementary Notes | | | | | |
| 16. Abstract Recent advances in GaAs bulk crystal growth using the LEC (liquid encapsulated Czochralski) technique are described. The dependence of the background impurity concentration and the dislocation density distribution on the materials synthesis and growth conditions were investigated. Background impurity concentrations as low as $4 \times 10^{15} \text{cm}^{-3}$ were observed in undoped LEC GaAs. The dislocation density in selected regions of individual ingots was very low, below the 3000cm^{-2} threshold. The average dislocation density over a large annular ring on the wafers fell below the 10^4cm^{-2} level for 3-inch diameter ingots. The diameter control during the program advanced to a diameter variation along a 3-inch ingot less than 2mm. | | | | | |
| 17. Key Words (Suggested by Author(s)) LEC GaAs Czochralski dislocation density high purity | | | | 18. Distribution Statement Approved for public release Distribution unlimited | |
| 19. Security Classif. (of this report) Unclassified | | 20. Security Classif. (of this page) Unclassified | | 21. No. of Pages 41 | |
| 22. Price* | | | | | |

* For sale by the National Technical Information Service, Springfield, Virginia 22161

TABLE OF CONTENTS

| | <u>Page</u> |
|--|-------------|
| 1.0 INTRODUCTION..... | 1 |
| 2.0 MATERIALS SYNTHESIS AND GROWTH TECHNIQUES..... | 6 |
| 2.1 Growth Configuration..... | 6 |
| 2.2 Growth Process..... | 6 |
| 2.3 Diameter Control..... | 8 |
| 3.0 CHARACTERIZATION TECHNIQUES..... | 13 |
| 3.1 Crystalline Perfection..... | 13 |
| 3.2 Impurity Characterization..... | 13 |
| 3.3 Electrical Transport Measurements..... | 17 |
| 4.0 RESULTS AND DISCUSSION..... | 21 |
| 4.1 Impurity Characterization..... | 21 |
| 4.1.1 SIMS AND LVM Impurity Studies..... | 21 |
| 4.1.2 Effect of H ₂ O in B ₂ O ₃ on Si and B..... | 24 |
| 4.1.3 Role of Oxygen..... | 26 |
| 4.2 Lattice Defect Studies..... | 26 |
| 4.2.1 Dislocations..... | 28 |
| 4.2.2 Peripheral Ga Inclusions..... | 31 |
| 4.2.3 Growth Techniques Affecting the Dislocation Density..... | 32 |
| 5.0 SUMMARY..... | 38 |

LIST OF FIGURES

| <u>Figure</u> | <u>Page</u> |
|---|-------------|
| 1. Large diameter undoped LEC GaAs ingot (R38/M) grown with manual diameter control to a tolerance better than 2 mm..... | 4 |
| 2. Cross section of the crucible for the LEC growth system, showing the location of the B_2O_3 during growth..... | 7 |
| 3. Cross section of the LEC crucible before growth showing the charge of elemental Ga and As and the preformed B_2O_3 disc..... | 9 |
| 4. Photograph of Si_3N_4 coracle in LEC system..... | 11 |
| 5. Diagram showing the neck, cone, and full-diameter sections of an LEC crystal..... | 12 |
| 6. Typical IR spectra showing C absorption..... | 16 |
| 7. PITS spectra for semi-insulating LEC GaAs, R4/C (Cr-doped) and R2/C (undoped) grown from SiO_2 crucibles..... | 19 |
| 8. Dependence of Si and B impurity levels on H_2O concentration in B_2O_3 encapsulant..... | 25 |
| 9. Photoluminescence spectra for undoped LEC GaAs ingots (R11,R16)..... | 27 |
| 10. Photograph of an etched (100) wafer showing fourfold symmetry pattern of dislocations..... | 29 |
| 11. Micrograph of the radial dislocation distribution for a 3-inch diameter (100) wafer from ingot R11/M..... | 30 |
| 12. Schematic of seed, neck, and top of cone showing variation in etch pit density due to seed necking (R16)..... | 36 |



| <u>Table</u> | <u>LIST OF TABLES</u> | <u>Page</u> |
|--------------|---|-------------|
| I. | Summary of Physical and Electrical Characteristics of LEC GaAs Crystals Grown Under NASA Program..... | 3 |
| II. | Typical Background Detection Sensitivity of Impurities Detected in LEC GaAs..... | 15 |
| III. | Summary of Major Traps Observed in LEC Materials by PITS..... | 20 |
| IV. | Baseline Purity in LEC GaAs..... | 23 |
| V. | SIMS Analysis of LEC GaAs..... | 23 |
| VI. | Summary of Etch Pit Results and Impact of Various Growth Techniques for LEC Ingots..... | 34 |



1.0 INTRODUCTION

The availability of large diameter GaAs substrates is essential for the production of low-cost, radiation hard solar cells. In the past, only Bridgman-grown GaAs substrates have been available, which are irregular in shape and dimension. The distribution of structural defects which can adversely effect the performance of solar cells is also non-uniform in these materials. While non-standard shapes and sizes are adequate for research and development of solar cell processing technology, large quantities of uniform wafers are necessary for low-cost, high yield production.

Recent advances in GaAs bulk crystal growth related to the development of the Liquid Encapsulated Czochralski (LEC) technique now make it possible to grow large diameter ingots. The purpose of the "Preparation of High Purity Low Dislocation GaAs Single Crystals" program (NAS3-22224) was to advance the LEC crystal growth technology to produce GaAs substrates for solar cell applications. Attention has been focused on two basic materials properties important to solar cells, background impurity levels and structural perfection. The dislocation density must be minimized to maintain the high minority-carrier diffusion lengths critical to good cell performance and radiation hardness. The background impurity concentration must be low to achieve semiconductor-quality electrical characteristics. We investigated the dependence of the concentration of background impurities and the density and distribution of dislocations on the materials synthesis and growth conditions.

Seven crystal growth experiments were performed at the Microelectronics Research and Development Center (MRDC) during the course of the program. Problems encountered during the growth of R19 forced termination

of the run before completion. Since six crystals were required to satisfy our contract requirements, an extra crystal (R38) was grown as a part of program. Information concerning the growth processes, and the physical and electrical characteristics are summarized in Table I. The results show that considerable progress was made during the program with respect to minimizing the concentration of background impurities, controlling the property of high resistivity, and minimizing the dislocation density. In the last three crystals grown during the program (R17,18,38), the sheet resistivity and dislocation density were higher than $1 \times 10^9 \Omega/\square$ and less than $1.8 \times 10^4 \text{ cm}^{-2}$, respectively. In one of these crystals (R17), the background impurities concentration ($N_D + N_A$), as low as $4 \times 10^{15} \text{ cm}^{-3}$ was achieved. The dislocation density in selected regions of some crystals was very low, below the 3000 cm^{-2} threshold. These overall properties are comparable, if not superior to those of commercial Bridgman material. In addition, the diameter control during the program advanced to a point where the diameter variation along a 3-inch ingot (R38) was less than 2 millimeters, as shown in Fig 1.

As a result of the progress attained during the NASA program, high-purity, undoped, 3-inch-diameter ingots with a diameter tolerance better than 2 millimeters are presently being grown. The material has the stable, semi-insulating characteristics required for GaAs IC's. Furthermore, the average dislocation density in the "ring" region of the substrates falls below the 10^4 cm^{-2} level at 3-inch diameter. These values are the lowest reported for 3-inch LEC crystals.

Table I
Summary of Physical and Electrical Characteristics of LEC GaAs Crystals
Grown on Contract NAS3-22224

| Rockwell I.D. No. | Crucible Material | Method of Diameter | Orientation | Crystal Diameter, mm | Crystal Length, cm | Crystal Weight Kg | $N_D + N_A, \text{cm}^{-3}$ | Sheet Resistivity, Ω/\square | Dislocation Density, at full Diameter, cm^{-2} |
|----------------------|----------------------|-----------------------|-----------------------|-------------------------|-----------------------|-------------------------|-----------------------------|--|---|
| 11 | SiO_2 | Manual | $\langle 100 \rangle$ | 63.1 ± 9.3 | 12 | 2.2 | 1.1×10^{16} | $< 10^7$ | 4×10^4 |
| 14 | SiO_2 | Coracle | $\langle 111 \rangle$ | 51.0 ± 1.0 | 23 | 1.9 | 7.1×10^{16} | $< 10^7$ | 2.3×10^4 |
| 16 | SiO_2 | Coracle | $\langle 111 \rangle$ | 51.0 ± 1.0 | 23 | 2.3 | 2.8×10^{16} | $> 10^9$ | --- |
| 17 | PBN | Manual | $\langle 100 \rangle$ | 72.2 ± 3.9 | 12 | 2.3 | 4×10^{15} | $> 10^9$ | 1.8×10^4 |
| 18 | PBN | Manual | $\langle 100 \rangle$ | 60.0 ± 8.5 | 16 | 1.7 | 1.5×10^{16} | $> 10^9$ | 1.0×10^4 |
| 19 | PBN | Manual | $\langle 100 \rangle$ | -- | -- | -- | -- | -- | --- |
| 38 | PBN | Manual | $\langle 100 \rangle$ | 80.0 ± 1.5 | 10 | 2.4 | 1×10^{16} | $> 10^9$ | 1.1×10^4 |



ORIGINAL PAGE
BLACK AND WHITE PHOTOGRAPH

MRDC81-15560

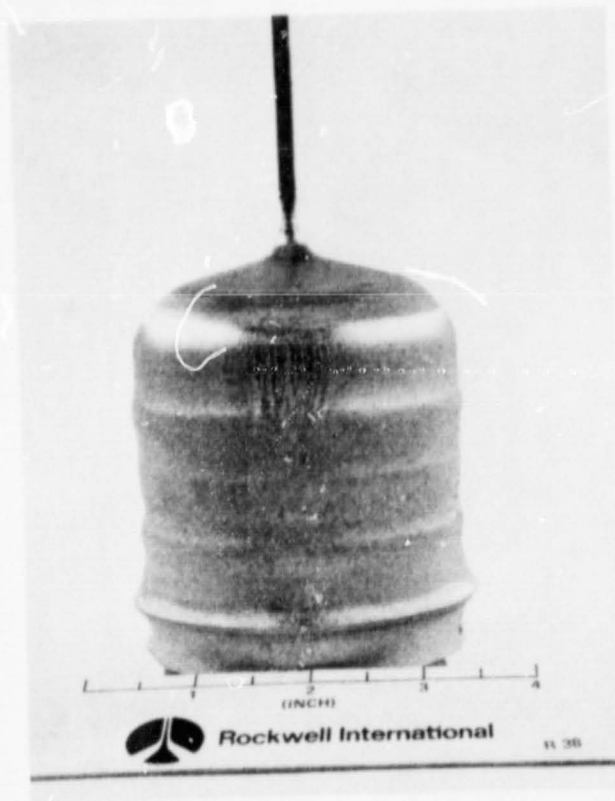


Fig. 1 Large diameter undoped LEC GaAs ingot (R38/M) grown with manual diameter control to a tolerance better than 2 mm.



This present capability of producing undoped, large-area, low-dislocation density material is extremely encouraging for the solar cell technology. Even lower dislocation densities are anticipated in doped materials since many dopants suppress the generation and multiplication of dislocations. Therefore it is expected that material can be produced with near-theoretical minority carrier diffusion lengths because the spacing between dislocations will be large compared with the mean-free-path of minority carriers. These high quality, large-area substrates will provide an excellent foundation for the production of efficient, cost-effective solar cells.

In this report, experimental results obtained on the NASA "Preparation of High Purity Low Dislocation Density GaAs Single Crystals" program are presented and discussed. In Section 2.0, the materials synthesis and growth techniques are outlined. In Section 3.0 the various techniques used to characterize the structural imperfections and chemical impurities are discussed. The cause-effect relationships between the crystal growth process and material properties are discussed in Section 4.0. The results are summarized and evaluated with respect to solar cell applications in the last section.

2.0 MATERIALS SYNTHESIS AND GROWTH TECHNIQUES

In this section, the processes involved in the materials synthesis and growth of LEC GaAs are described.

2.1 Growth Configuration

All crystals were grown in Rockwell International's Melbourn high-pressure LEC system at the Thousand Oaks MRDC laboratory. The configuration of the LEC system, shown schematically in Fig. 2, consists of a GaAs melt contained in either a high purity quartz (Metals Research) or pyrolytic boron nitride (Union Carbide) crucible. The boric oxide (B_2O_3) encapsulant floats on the top surface of the melt. In addition, a thin film of B_2O_3 coats the entire surface of the crucible due to the high-temperature wetting characteristics of the materials. The B_2O_3 also wets the growing crystal. Thus, the GaAs melt is completely sealed suppressing As evaporation and shielding the melt against contamination from the crucible and the growth ambient.

2.2 Growth Process

The major steps in the crystal growth operation included loading of the charge, heat up, synthesis, equilibration, seeding, necking, cone growth, and pulling of the full-diameter ingot. The crucible was loaded with approximately 1400g 6-9's Ga (Ingal International), 1500g 6-9's As (Cominco), and a 500g preformed B_2O_3 disk (Puratronic) with a known moisture content, as shown

MRDC81-11822

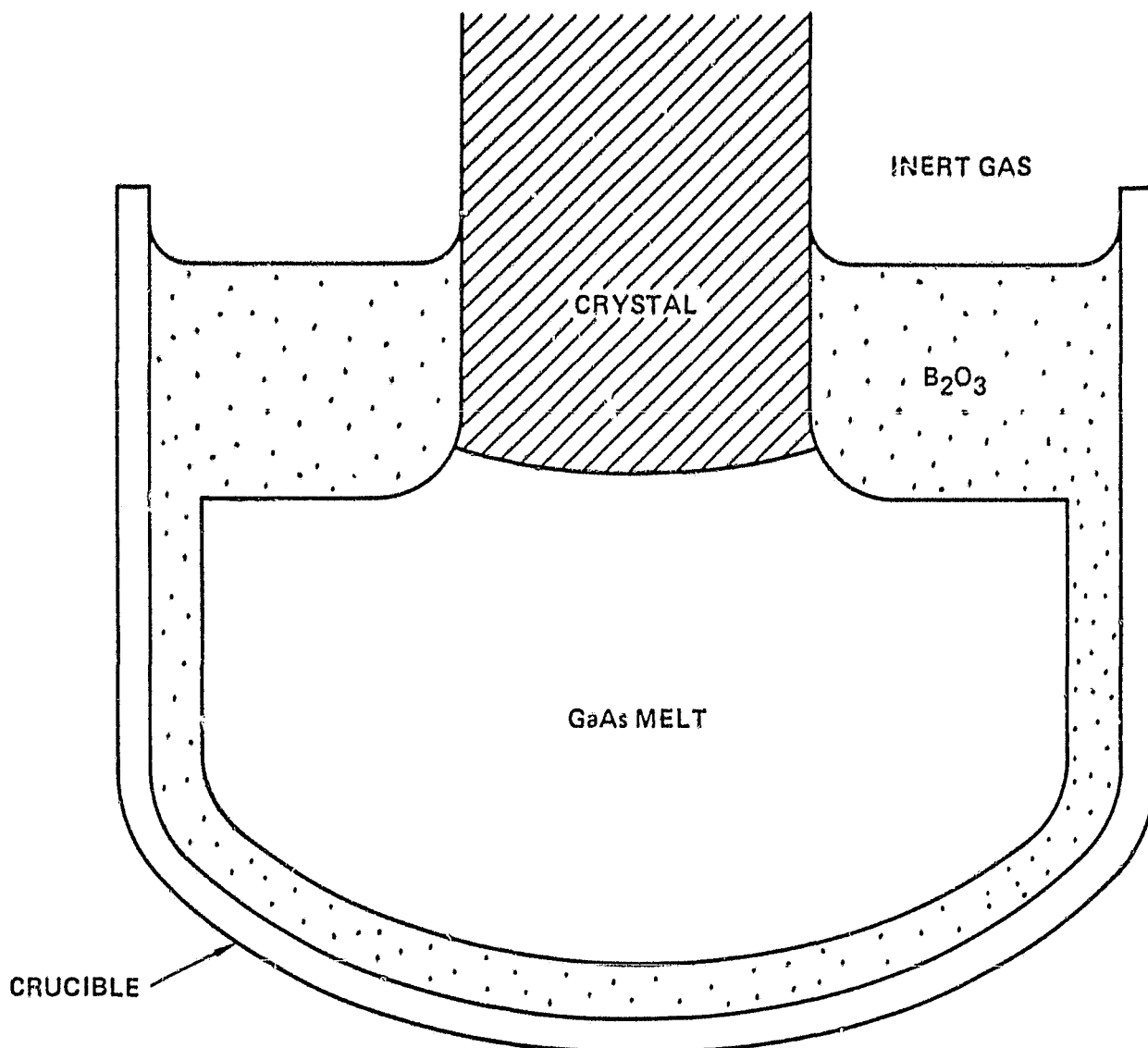


Fig. 2 Cross section of the crucible for the LEC growth system, showing the location of the B₂O₃ during growth.

in Fig. 3. Ga, which is solid to just above room temperature, was loaded on top of the As so that the liquid Ga served to encapsulate the As. Starting with a chamber pressure of 600 psi, the crucible was heated to between 450 and 500°C, at which point the B_2O_3 melted, flowed over the charge of Ga and As, and sealed at the crucible wall. The synthesis reaction ($Ga_{liquid} + As_{solid} = GaAs_{solid}$) occurred at about 860°C. The presence of the B_2O_3 and the use of high overpressures (~ 1000 psi) prevented significant loss of As due to sublimation and evaporation during and subsequent to synthesis. The melt was then equilibrated at the starting temperature and the growth procedure begun.

Growth was initiated by dipping the seed, which was held on the pull shaft, through the B_2O_3 and into the melt. The crystal was grown by gradually withdrawing the seed from the melt. The diameter was gradually and controllably increased to full dimension. The seed and the crucible were rotated in the same direction at 6 and 15 rpm, respectively.

2.3 Diameter Control

The diameter of the crystal was controlled either by manual operation or through the use of the coracle shaper. Using manual control the crystal diameter was monitored through the differential weight signal. This signal was obtained from the "load cell," a special weighing device on which the crystal and pull shaft are mounted in the LEC system. An increase or decrease of the differential weight indicates a corresponding increase or decrease in diameter. The crystal diameter was controlled by varying the heater temperature and the cooling rate in response to changes in the differential weight signal.

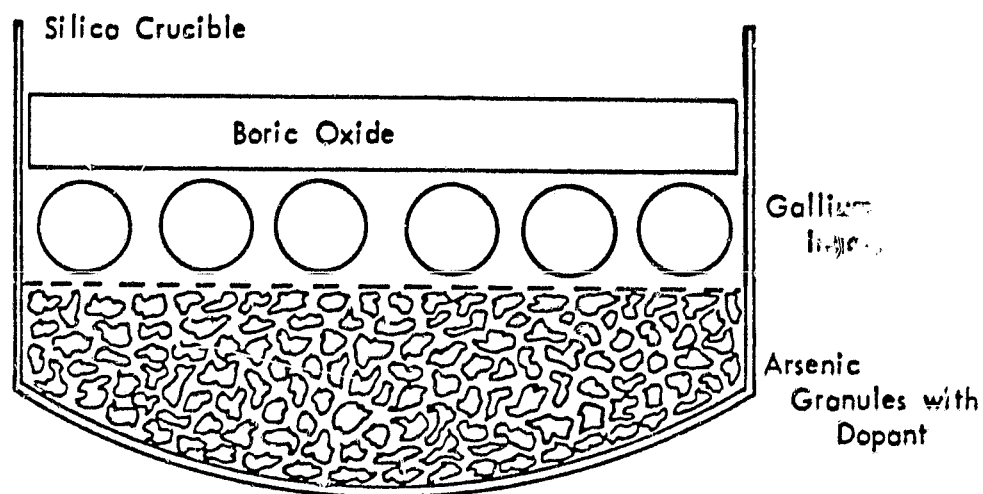


Fig. 3 Cross section of the LEC crucible before growth showing the charge of elemental Ga and As and the preformed B_2O_3 disc.



The coracle, shown in Fig. 4, is a Si_3N_4 die with a round hole in the center. The coracle floats on top of the GaAs melt. A crystal pulled from the melt through the die has exceedingly good diameter control. However, the use of the coracle seems to be limited to growth in the $\langle 111 \rangle$ direction because other low index planes, such as (100), show a high susceptibility to twinning. It is important to note that the LEC system is equipped with a Vidicon camera for optical viewing of the growth process. The growth process is monitored continuously in this way to ensure stable control. Also, under certain circumstances, the differential weight signal does not accurately represent the actual variation of the diameter making visual monitoring essential.

The crystals were grown in three different sections with respect to diameter, as illustrated in Fig. 5. After the seed was dipped into the melt and pulling had begun, the "neck" was formed by reducing the diameter of the crystal below the diameter of the seed (~ 4 millimeters) to from 1 to 3 millimeters. Then the diameter was gradually and controllably increased forming the "cone." When the diameter of the cone reached the desired dimension, the diameter of the crystal was kept constant for the remainder of the growth run. The dependence of density and distribution of dislocation on the neck diameter, neck length, and cone angle was investigated.

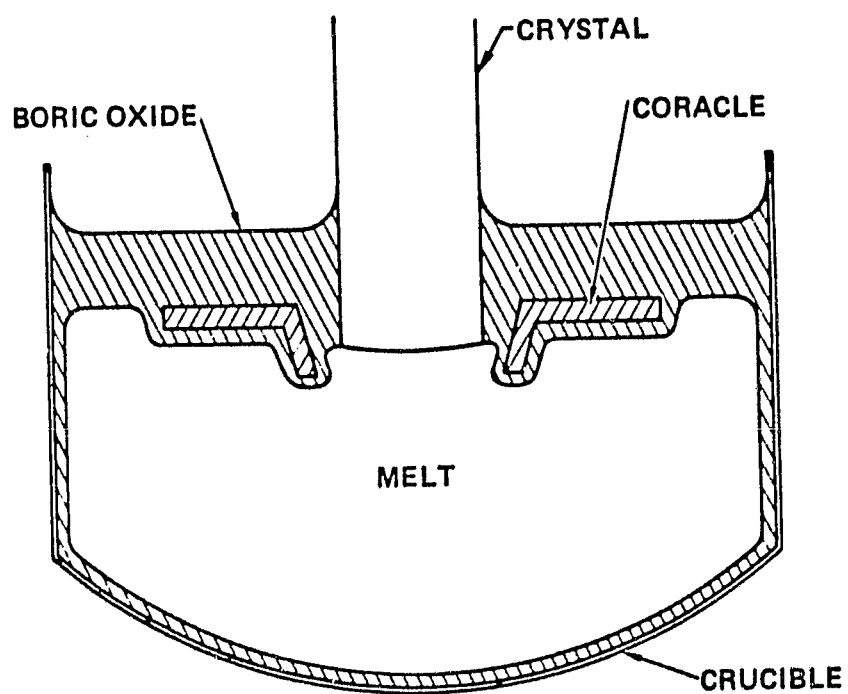


Fig. 4 Photograph of Si₃N₄ coracle in LEC system.



ORIGINAL PAGE
BLACK AND WHITE PHOTOGRAPH

MRDC81-15561

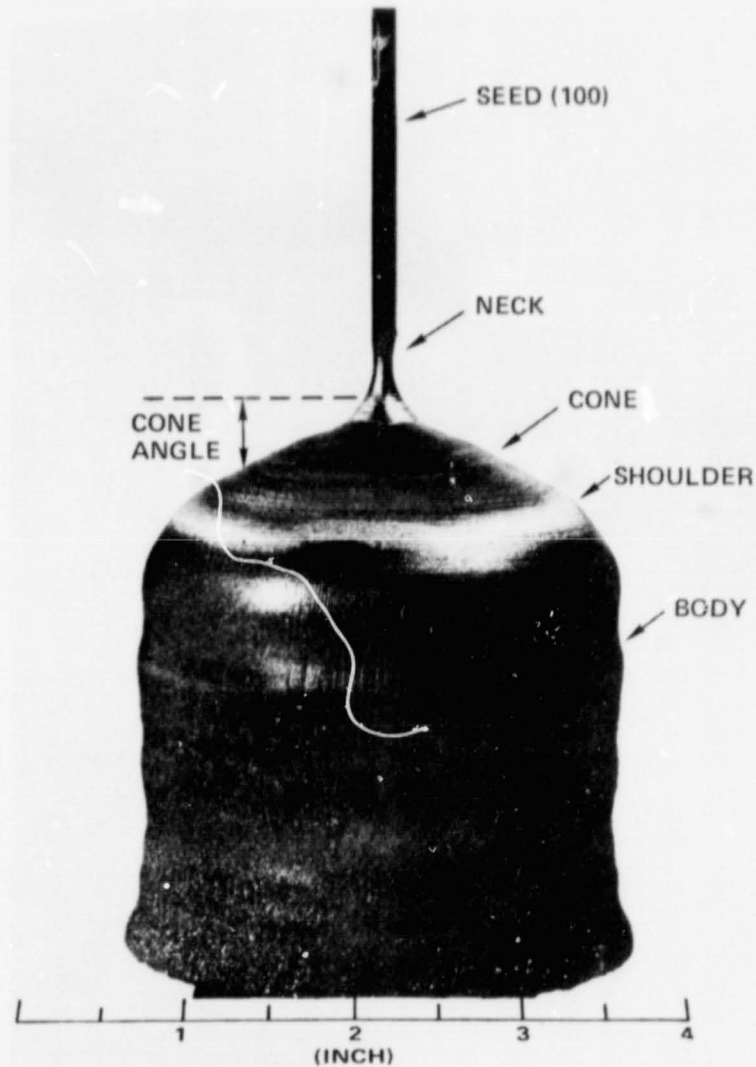


Fig. 5 Diagram showing the neck, cone, and full-diameter sections of an LEC crystal.

ORIGINAL PAGE
BLACK AND WHITE PHOTOGRAPH

3.0 CHARACTERIZATION TECHNIQUES

This section briefly reviews the analytical techniques used to characterize the LEC material in terms of crystalline perfection, chemical impurities, and electrical and optical properties.

3.1 Crystalline Perfection

The crystalline perfection of the LEC crystals was evaluated by determining the density and distribution of dislocations. Dislocations act as recombination centers and reduce the minority-carrier lifetime. The dislocation densities of (100) wafers were measured by etching polished wafers in KOH for 25 min at 400°C. This etch preferentially attacks dislocations that intersect the surface of the wafer. A $\text{HNO}_3:3\text{H}_2\text{O}$ etch was used to determine dislocation densities for (111) wafers. The density of etch pits corresponds directly to the density of dislocations. Back reflection x-ray topography also aided in analyzing the distribution of dislocations.

3.2 Impurity Characterization

The following is a list of brief descriptions of techniques used to analyze background impurities in the LEC material.

Secondary Ion Mass Spectrometry (SIMS)

SIMS measurements were made at Charles Evans and Associates, San Mateo, CA. This is a chemically specific micro-analytical technique

particularly well suited for transition metals and shallow donors in GaAs. The system is calibrated against ion implanted standards. The typical background detection sensitivity (the concentration below which measurements are not meaningful) of the impurities analysed during this program are given in Table II. Although the detection sensitivity is very low for these impurities, making SIMS an excellent tool for the characterization of GaAs, the measured impurity concentration of an element in LEC GaAs is often close to the background sensitivity. Since the background sensitivity can vary from day to day (as indicated in the table), the background sensitivity was checked against a high purity standard before these analyses were made.

Local Vibrational Mode (LVM) Infrared Absorption

LVM measurements have been demonstrated to be an effective and nondestructive method for identifying low-Z impurities in GaAs, particularly for Al, B, C, Li, Si and O₂. Measurements of the carbon-induced LVM band have been carried out for samples cut from several undoped LEC ingots. The IR absorption for ¹²C occurs at $\nu = 582 \text{ cm}^{-1}$. A typical IR spectra showing the C absorption is shown in Fig. 6. The technique is well suited determining the relative concentration of carbon in different samples. However, the absolute accuracy of the technique is uncertain and considerable error can arise in measuring low concentrations of C in conducting material.

Table II

Typical Background Detection Sensitivity of Impurities Detected in LEC GaAs

| Element | Si | S | Se | Te | B | Mg | Cr | Mn | Fe |
|--|-----------|--------|-----------|--------|------|-----------|-----------|-----------|-----------|
| Background Detection Sensitivity (cm^{-3}) | 3E14-1E15 | 1-2E15 | 1E12-1E14 | 1-5E13 | 5E13 | 1E14-1E15 | 1E14-1E15 | 5E14-2E15 | 1E15-1E16 |

ANALYSIS OF CARBON IN LEC GaAs
BY LOCALIZED VIBRATIONAL MODE
TECHNIQUE AT 77°K (R11/M)

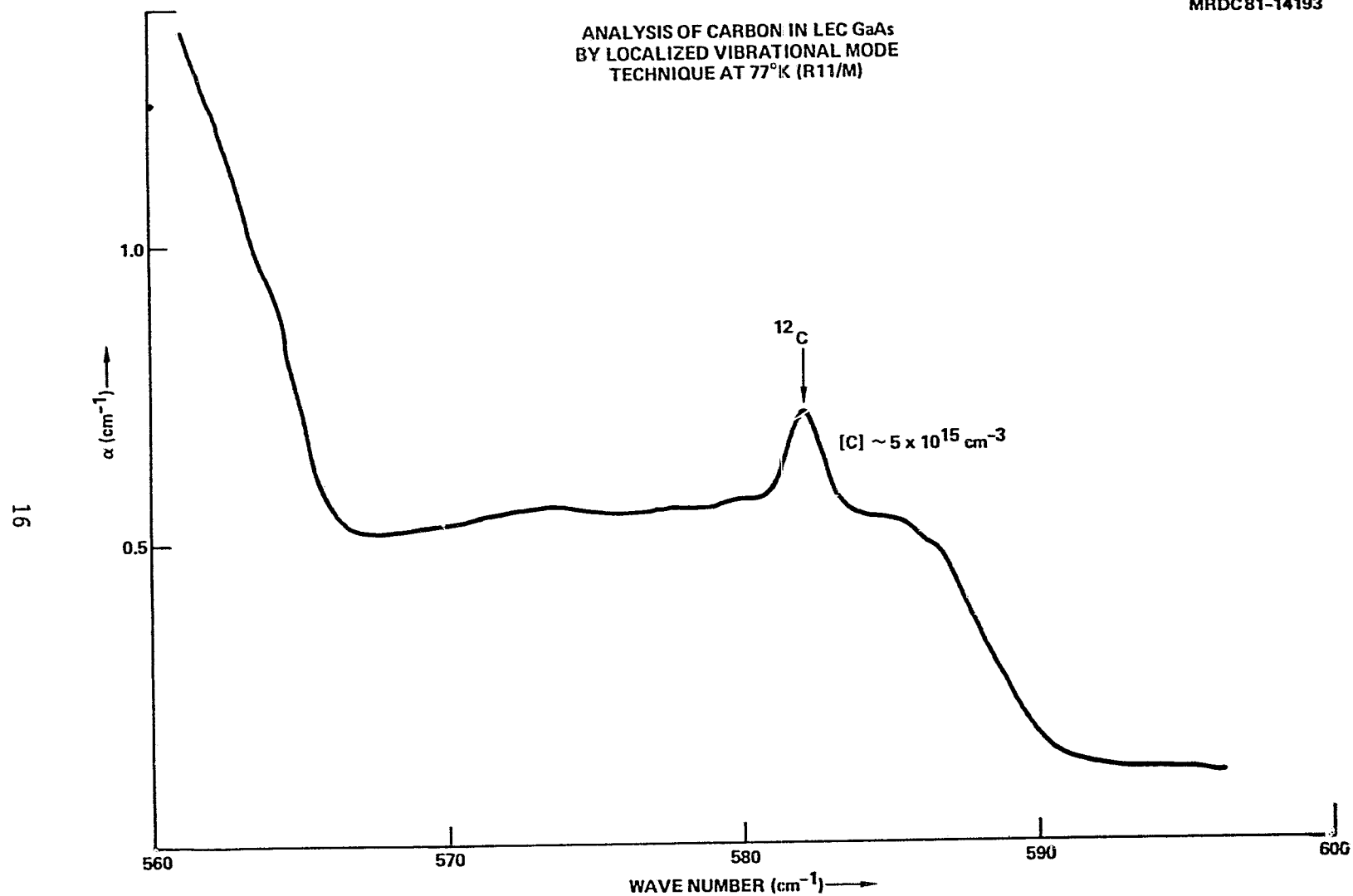


Fig. 6 Typical IR spectra showing C absorption.



Photoluminescence

Low temperature (4.2K) photoluminescence measurements have been made on MRDC LEC material by Dr. Phil Yu at Wright State University, Dayton, Ohio. This is a very sensitive optical technique particularly well suited for analyzing deep levels in GaAs.

3.3 Electrical Transport Measurements

Electrical transport measurements have been carried out to characterize the dominant electrical centers in the LEC material and to determine the chemical origin of these centers by comparing the results with chemical analyses. Hall measurements, capacitance-voltage (C-V) profiling, and Photo-Induced Transient Current Spectroscopy (PITS), which was developed at Rockwell MRDC, have been utilized in these studies. PITS is used to characterize deep levels in semi-insulating material. In addition, as a part of MRDC's IR&D work, Deep-Level Transient Spectroscopy (DLTS) was performed by Dr. Kang Wang at the University of California at Los Angeles. DLTS is used to characterize deep levels in conducting and ion implanted material, complimenting the PITS technique used to characterize semi-insulating materials.

Over the last several years, substantial development of the PITS technique has been undertaken at Rockwell MRDC for the evaluation of trap energies and emission rates in semi-insulating materials. The PITS technique deals with the rise and decay of photocurrents rather than with capacitance transients as in DLTS. Many of the trapping levels detected in earlier work



have been correlated with reports in the literature, substantiated with alternate measurement techniques, and confirmed by doping experiments. Figure 7 shows, for illustration, a composite PITS spectra from semi-insulating GaAs samples, a Cr-doped (R4/C) and an undoped (R2/C), which were all grown from SiO_2 crucible. The PITS response is represented as $\Delta I/I_0$, normalized to the photo-current I_0 vs absolute temperature. The broad $E_v + 0.89$ eV peak observed in the Cr-doped samples was associated with Cr^{+2} acting as a hole trap. The PITS signal at 290K has been associated with a hole trap from Fe located at $E_v + 0.52$ eV. Correlation with 4K photoluminescence and reports in the literature have revealed that an impure Cr source may be responsible for Fe doping. Figure 7 shows an absence of the 0.52 eV level in the undoped ingot R2/C. A very common electron trap at 190K ($E_v + 0.34$ eV), which is associated with the presence of Cr, is also shown in Fig. 7. All undoped GaAs did not show the 0.34 eV level in spectra, whereas all Cr-compensated crystals, without exception, exhibited it. The assignment of the 0.34 eV level has not been made directly to a Cr site but the center could involve a complex with Cr. Very low PITS signals observed near the low absolute temperature range for both samples were also consistent with SIMS results in which low shallow-donor impurity (such as Si) levels were observed. The 0.65 eV level could be related to the presence of O. Table III summarizes all major trap levels observed in MRDC LEC material as determined by PITS and DLTS.

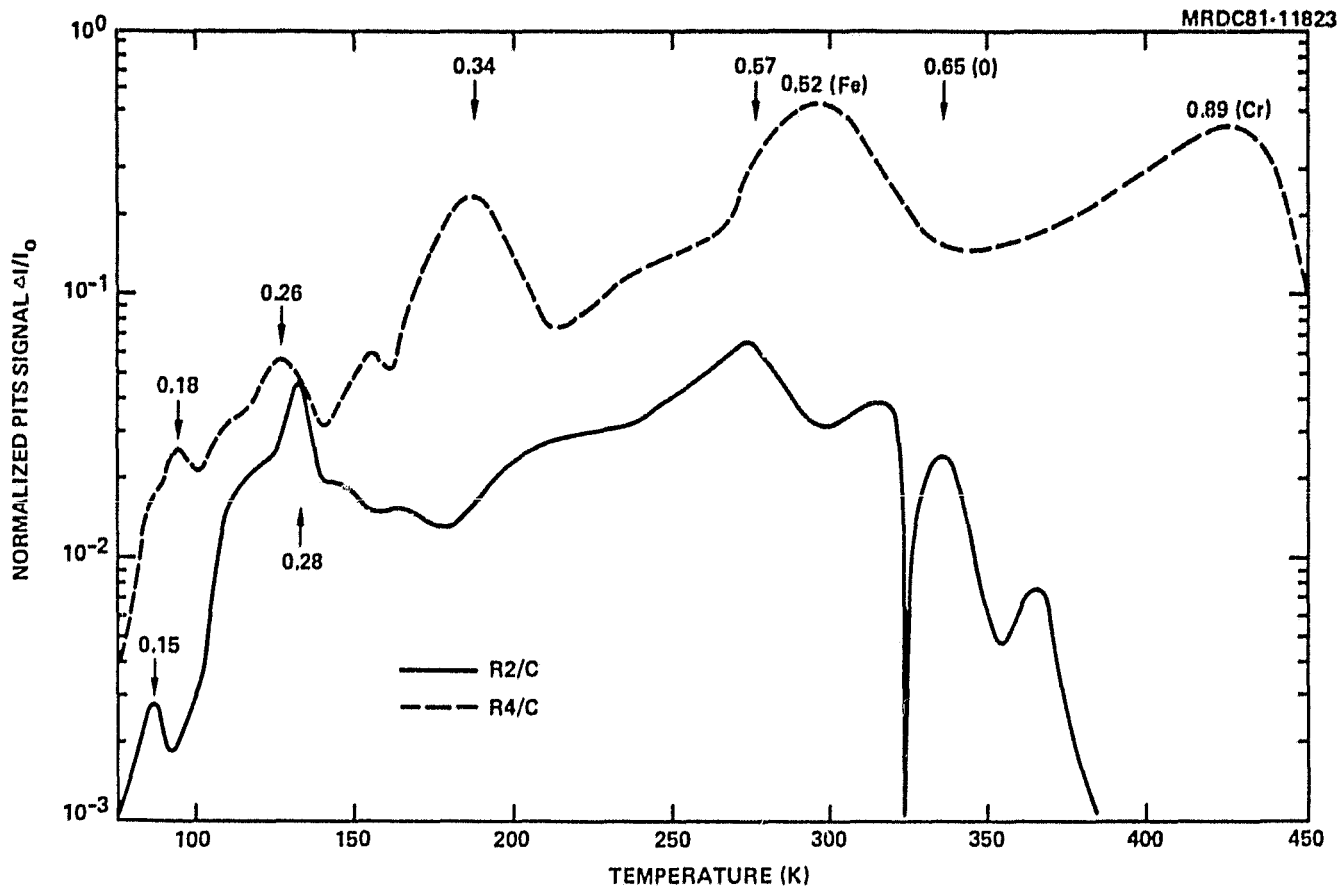


Fig. 7 PITS spectra for semi-insulating LEC GaAs, R4/C (Cr-doped) and R2/C (undoped) grown from SiO_2 crucibles

Table III

Summary of Major Traps Observed in LEC Materials by PITS

| $T_m(K)$ (@ 3 msec) | $E_t(eV)$ | $\sigma(cm^2)$ | Identity | Comments |
|------------------------|-----------|------------------------|----------|-----------------|
| 188 | 0.34 | $4 \times 10^{-14}(n)$ | EL7 | Cr-Doped |
| 274 | 0.57 | $6 \times 10^{-13}(n)$ | EL3 | - |
| 283 | 0.52 | $1 \times 10^{-15}(p)$ | HL8 | (Fe)Cr-Doped |
| 335 | 0.65 | $8 \times 10^{-14}(n)$ | - | (O) |
| 373 | 0.83 | $2 \times 10^{-13}(p)$ | HL10 | Low H_2O |
| 430 | 0.89 | $4 \times 10^{-14}(p)$ | HL1 | (Cr) |
| - | 0.74 | - | EL2 | Dark Cond. DLTS |

4.0 RESULTS AND DISCUSSION

The results of impurity electrical and crystallographic studies undertaken on LEC GaAs are described in this section.

4.1 Impurity Characterization

4.1.1 SIMS and LVM Impurity Studies

The concentrations of background shallow-donor (Si, S, Se, and Te) and metal (Mg, Cr, Mn, Fe, and B) impurities as determined by SIMS measurements are shown in Table IV. With the exceptions Si, B, and Mg, which will be discussed in more detail below, the concentration levels are exceedingly low. Many readings are either at or below the typical background sensitivity (see Table II) of the SIMS technique, suggesting that LEC material in some cases is purer element-by-element than the standard used to check the SIMS background sensitivity. The relatively high concentrations of Fe in R16 and R18 are attributed to high background levels present during those particular measurements. In no instance was the measured level greater than the background level by more than about a factor of 2.

LVM measurements of C in the NASA crystals displayed considerable variations. The concentration of C in R11 and R17 was less than $5 \times 10^{15} \text{ cm}^{-3}$, whereas the C concentration in R14 was about $3 \times 10^{16} \text{ cm}^{-3}$. The high concentration of C could be related to the presence of the coracle floating on the melt; further investigations are underway. In addition, published reports

giving the absorption cross-section of C in GaAs are being carefully re-examined. The absorption cross-section determines the calibration of the measurement. The reported value should be confirmed to raise the certainty of the measurements.

To take full advantage of the impurity analysis performed on the NASA contracts, the results obtained from the NASA crystals were averaged with those obtained from crystals grown on the MRDC IR&D program. The combined results are shown in Table IV. The impurity analyses for individual NASA ingots are shown in Table V. The crystals are categorized in terms of the crucible material and the technique used for diameter control. Results obtained from four Bridgman crystals, which passed internal qualification tests for GaAs IC processing, are provided for comparison.

Three conclusions were drawn from the results of the combined impurity analysis.

1. The background concentration of the transition metals Cr, Mn, and Fe in undoped LEC GaAs grown from quartz and PBN crucibles is generally less than about $2 \times 10^{15} \text{ cm}^{-3}$. C, on the other hand, is present at levels varying from about 3×10^{15} to $3 \times 10^{16} \text{ cm}^{-3}$. Therefore, C is expected to be one of the dominant acceptors in LEC material. The background concentration of the shallow donors S, Se, and Te are also typically less than $2 \times 10^{15} \text{ cm}^{-3}$.
2. Mg and C contamination seem to be related to the presence of the Si_3N_4 coracle in the crucible. An impurity analysis on the coracle material is underway.



Table IV
Baseline Purity in LEC GaAs

| GROWTH TECHNIQUE | CRUCIBLE | NUMBER OF CRYSTALS AVERAGED | S | Se | Te | Mg | Cr | Mn | Fe | C |
|------------------------|----------|-----------------------------|------|--------|-------|---------|--------|----------------------|----------------------|--------------|
| LEC | Quartz | | | | | | | | | |
| | Manual | 6 | 2e15 | <1e15 | <1e14 | <5e14 | <5e14 | <1e15 | <9e ¹⁵ | ~ 3e15 |
| | Coracle | 7 | " | " | " | 2-10e15 | " | " | " | ~ 2e16 |
| LEC | PBN | | | | | | | | | |
| | Manual | 3 | 1e15 | 7e13 | 2e13 | 3e14 | 1e15 | 1e15 | 2e15 | ~7e15 |
| | Coracle | 1 | 2e15 | 1.5e14 | <1e14 | 4.4E14 | 8.5e15 | 1.5e15 | <5e15 | ~2e16 |
| Bridgman (Cr-doped) | Quartz | 4 | 3e15 | 3E14 | 4E13 | 4.5E14 | 3.1E16 | 4.7x10 ¹⁴ | 3.1x10 ¹⁵ | Not Detected |

Table V
SIMS Analysis of LEC GaAs

| Sample No. | Impurity Concentration (cm ⁻³) | | | | | | | | | Approximate H ₂ O Concentration in B ₂ O ₃ , ppm |
|------------|--|--------|--------|--------|--------|--------|--------|--------|--------|---|
| | Si | S | Se | Te | Mg | Cr | Mn | Fe | B | |
| R11 F | 5.0E15 | 1.0E15 | <E14 | <E14 | 2.E14 | 6.0E14 | 5.0E14 | 4.0E14 | 9.0E15 | 500 |
| R11 T | 4.0E15 | 2.0E15 | <E14 | <E14 | 2.0E14 | 5.0E14 | 8.0E14 | 4.0E15 | 1.0E16 | " |
| R14 F | 3.0E16 | 2.0E15 | 2.0E14 | <E14 | 1.0E16 | 3.0E14 | 4.0E14 | 2.0E15 | 2.0E17 | 200 |
| R14 T | 3.0E16 | 2.0E15 | 1.0E14 | <E14 | 1.0E16 | 4.0E14 | 6.E14 | 3.0E15 | 2.0E17 | " |
| R16 F | 1.0E15 | 5.0E15 | 2.0E14 | 1.0E14 | 2.0E15 | 7.0E14 | 2.0E15 | 6.0E15 | 7.0E15 | 1000 |
| R16 T | 4.0E14 | 5.0E15 | 1.0E14 | <E14 | 1.0E15 | 3.0E15 | 2.0E15 | 2.0E16 | 6.0E14 | " |
| R17 F | 2.0E14 | 5.0E14 | <E14 | <E14 | <E14 | 2.0E14 | 1.0E15 | 8.0E14 | 2.0E16 | 520 |
| R17 T | 1.0E14 | 1.0E15 | 3E14 | <E14 | 1.0E14 | 1.0E14 | 1.0E15 | 1.0E15 | 1.0E17 | " |
| R18 F | 3.0E14 | 3.0E15 | 2.0E14 | <E14 | 4.0E14 | 7.0E14 | 1.0E15 | 5.0E15 | 5.0E16 | 450 |
| R18 T | 3.0E14 | 1.0E15 | 1.0E14 | <E14 | 5.0E14 | 1.0E15 | 2.0E15 | 1.0E16 | 5.0E16 | " |
| R38 F | 2.0E14 | 4.0E14 | <E14 | <E14 | 4.0E14 | 6.0E14 | 8.0E14 | 5.0E15 | 2.0E16 | 500 |
| R38 T | 2.0E14 | 6.0E14 | <E14 | <E14 | 4.0E14 | 8.0E14 | 1.0E15 | 5.0E15 | 2.0E17 | " |



3. The important difference between LEC and Bridgman material with respect to the impurities in Table V is the presence of C in LEC material. This understanding could be important to the evaluation of the device performance of LEC material.

4.1.2 Effect of H₂O in B₂O₃ on Si and B

The concentration of both Si and B in the NASA crystals (see Table VI) were variable, ranging from 1×10^{14} to 3×10^{16} cm⁻³ and 6×10^{14} to 2×10^{17} cm⁻³, respectively. Since Si is a shallow donor, it is particularly important to understand how Si becomes incorporated in the crystal.

Comparing the impurity analysis of R14 and R16, it was observed that the concentration of Si in crystals grown from quartz crucibles, and the concentration of B in crystals grown from both quartz and PBN crucibles increased as the concentration of H₂O in the B₂O₃ encapsulant decreased. To obtain adequate statistics to characterize this behavior, in Fig. 8 the Si and B concentration of 13 crystals grown on both the NASA and IR&D programs were averaged.

Figure 8 shows a pronounced dependence of the Si and B levels on the concentration of H₂O. The variability of the Si and B in the NASA crystals is attributed to this behavior. The results show that H₂O in the encapsulant reduces the transport of Si through the B₂O₃ from the quartz crucible to the melt. In addition, the presence of H₂O reduces the pick-up by the melt of B from the B₂O₃. B contamination from the PBN crucible appears to be insignificant. The exact mechanism associated with the action of H₂O is presently under investigation.

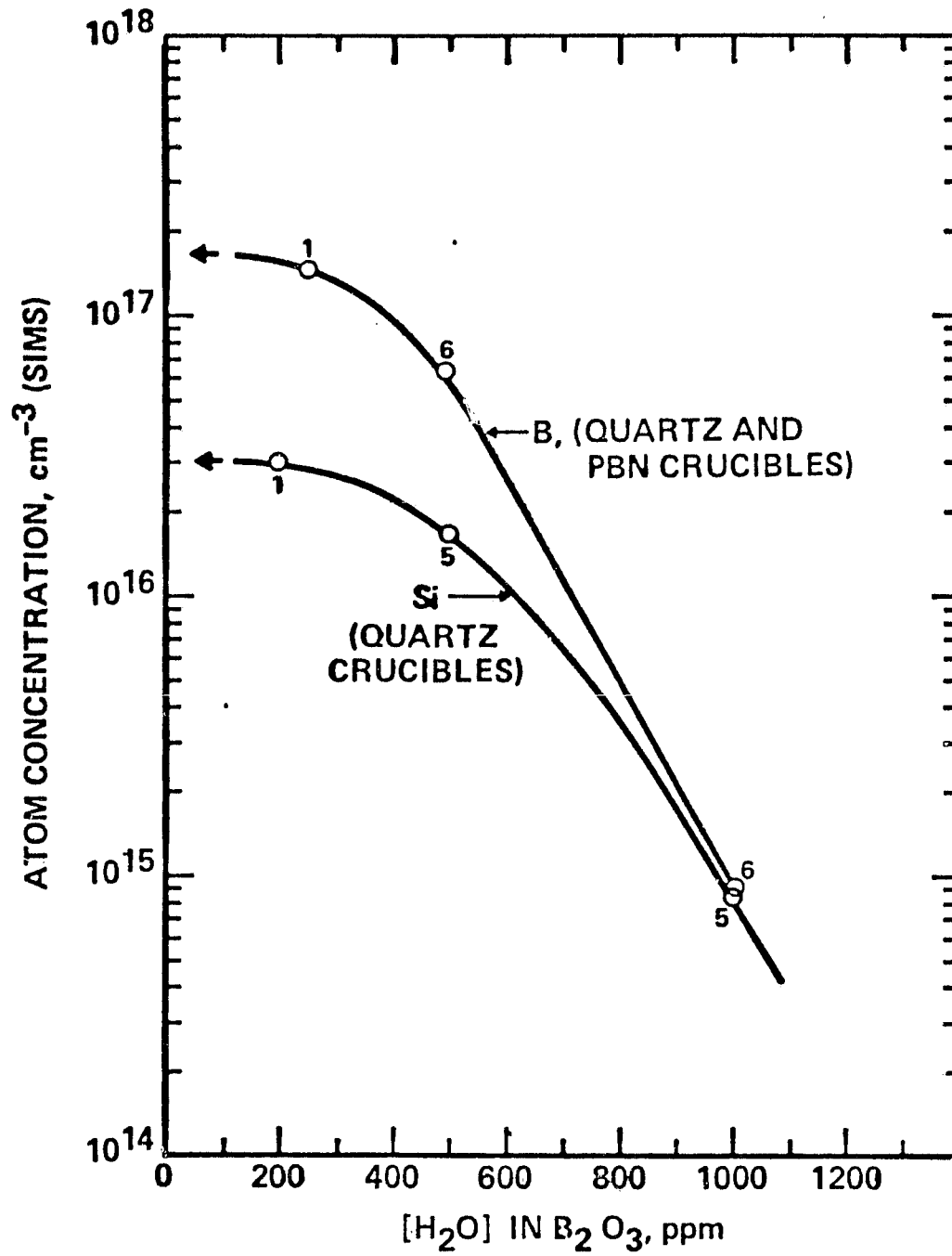


Fig. 8 Dependence of Si and B impurity levels on H_2O concentration in B_2O_3 encapsulant

4.1.3 Role of Oxygen

The characterization of O in GaAs has been an area of considerable interest and some controversy for several years. The understanding of the behavior of O is important for the development of microwave devices in particular because deep donor centers at 0.65 and 0.75 eV, which could control the semi-insulating properties of LEC GaAs, could be related to O or O-defect complexes. This is an area of great interest at the present time.

PITS and photoluminescence measurements have been made on LEC crystals grown during the NASA and IR&D programs. An important feature of the PITS spectra (see Fig. 6) is a peak associated with an electron trap located 0.65 eV below the conduction band. Photoluminescence spectra of the NASA crystals, shown in Fig. 9, contain a corresponding peak at 0.65 eV. The intensity of the peak is highest in material grown with "wet" B₂O₃. This observation suggests the possibility that the concentration of the 0.65 eV deep donor is related to O, and, that the concentration of the center is controlled by the moisture content of the encapsulant. Further investigations are underway.

4.2 Lattice Defect Studies

Structural defects in LEC material were characterized by preferential etching, and optical, Infrared (IR), and Transmission Electron (TEM) Microscopy. The results show that the material is essentially free of stacking faults, precipitates, inclusions, and low-angle grain boundaries. Further, the principal defects were identified as dislocations and peripheral Ga inclusions.

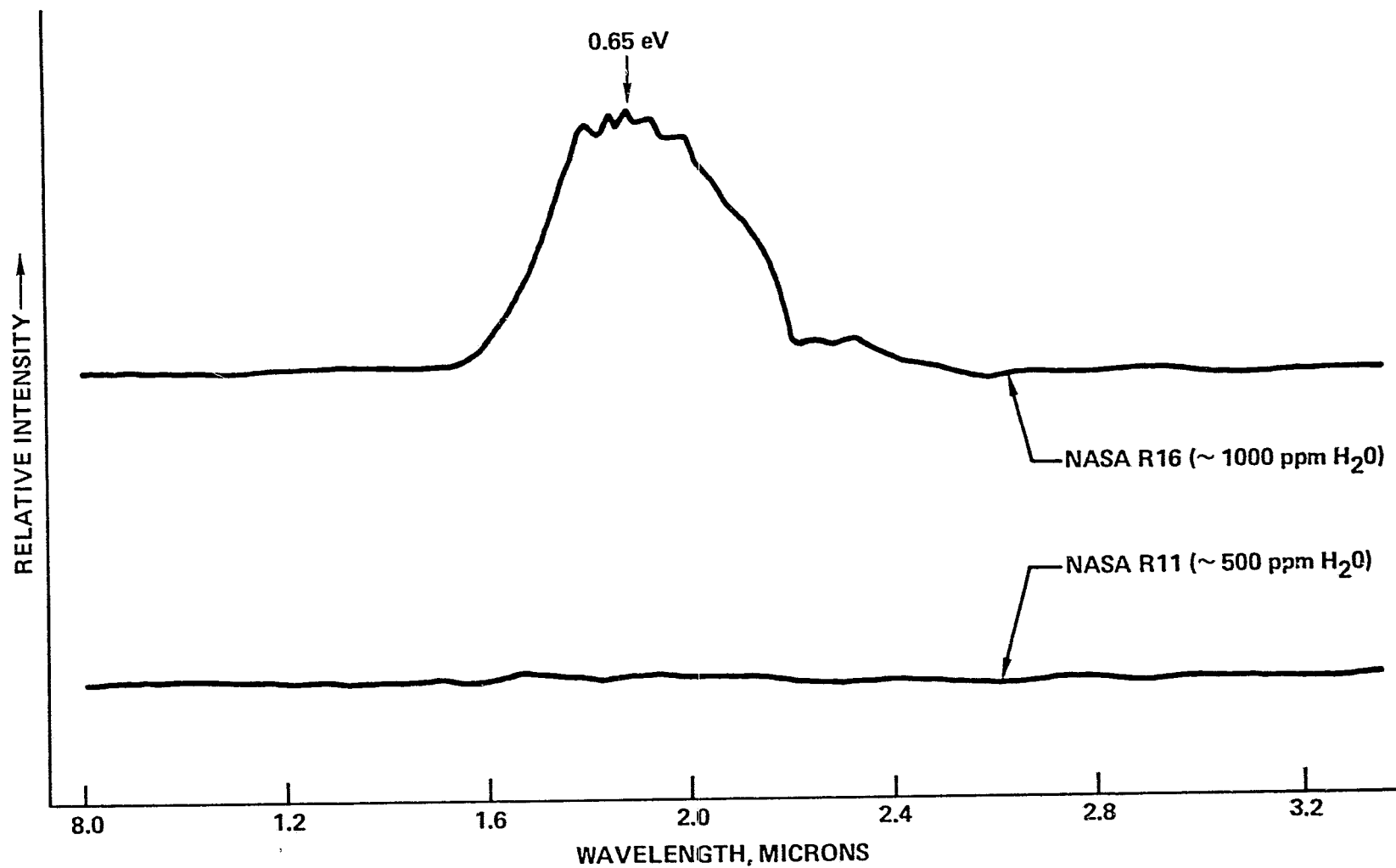


Fig. 9 Photoluminescence spectra for undoped LEC GaAs ingots (R11,R16)



4.2.1 Dislocations

Radial and longitudinal dislocation distributions in LEC ingots

The crystalline perfection of the LEC crystals was evaluated by determining the dislocation density and distribution. Both chemical etching techniques and x-ray reflection topography measurements were applied to polished LEC wafers. In general, exactly the same patterns were obtained by both techniques. Since the chemical etching technique offer the advantages of easy sample preparation, speed, and good resolution, the efforts in the present study were based on this technique. The detail of experimental procedures for this technique have been described in section 3.0.

The distribution of dislocations across KOH-etched wafers exhibited symmetry indicative of the crystallographic orientation. A photograph of an etched (100) wafer taken from the front of an LEC ingot is shown in Fig. 10. The etch pattern has fourfold symmetry. The etch pattern on (111) wafers displayed three-fold symmetry. A microscopic view of the dislocation distribution on a 3-in diameter (100) wafer is shown in Fig. 11. This composite photomicrograph clearly illustrates the large variation in the radial distribution of dislocations depicted in Fig. 10. The features of the dislocation distribution are: (1) minimum density occurs over a large area between the center and edge (Region 1; "ring"); (2) intermediate density occurs in the center (Region 2; "center"); (3) maximum density occurs in a 0.2 in. wide area around the edge (Region 3; "edge"). In addition, the density at the edge along the $\langle 100 \rangle$ direction is greater than that along the $\langle 110 \rangle$ direction. The observed etch patterns reported here are shown to be consistent with recent theoretical



ORIGINAL PAGE
BLACK AND WHITE PHOTOGRAPH

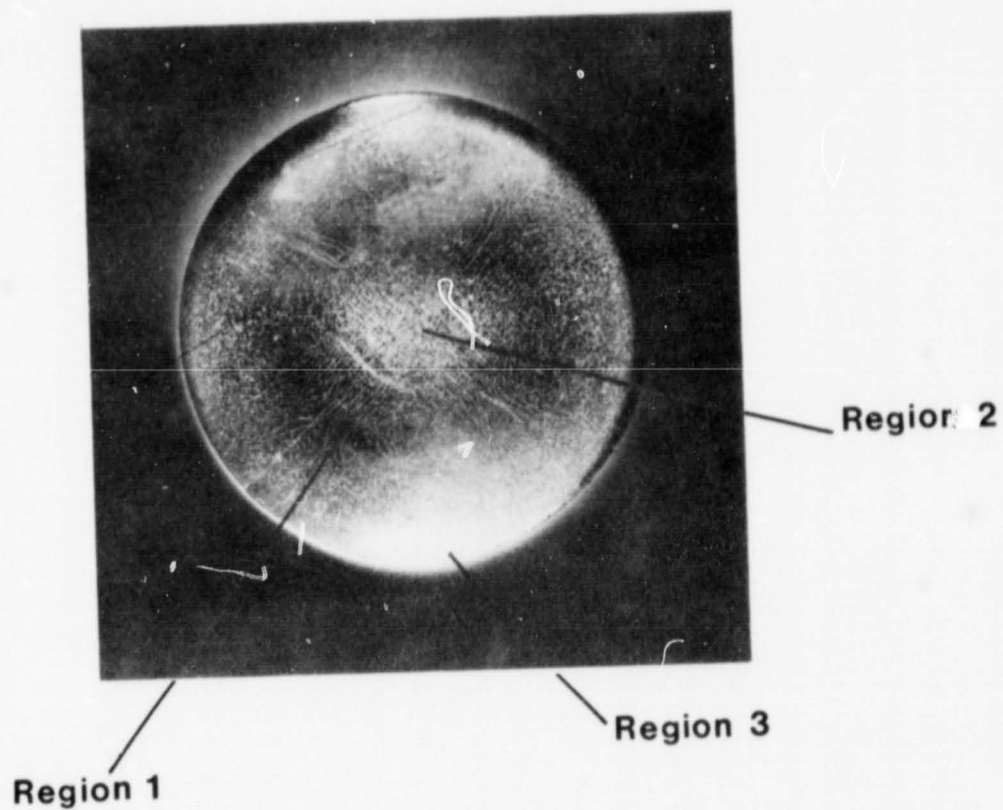


Fig. 10 Photograph of an etched (100) wafer showing fourfold symmetry pattern of dislocations.



ORIGINAL PAGE
BLACK AND WHITE PHOTOGRAPH

MRDC81-14195

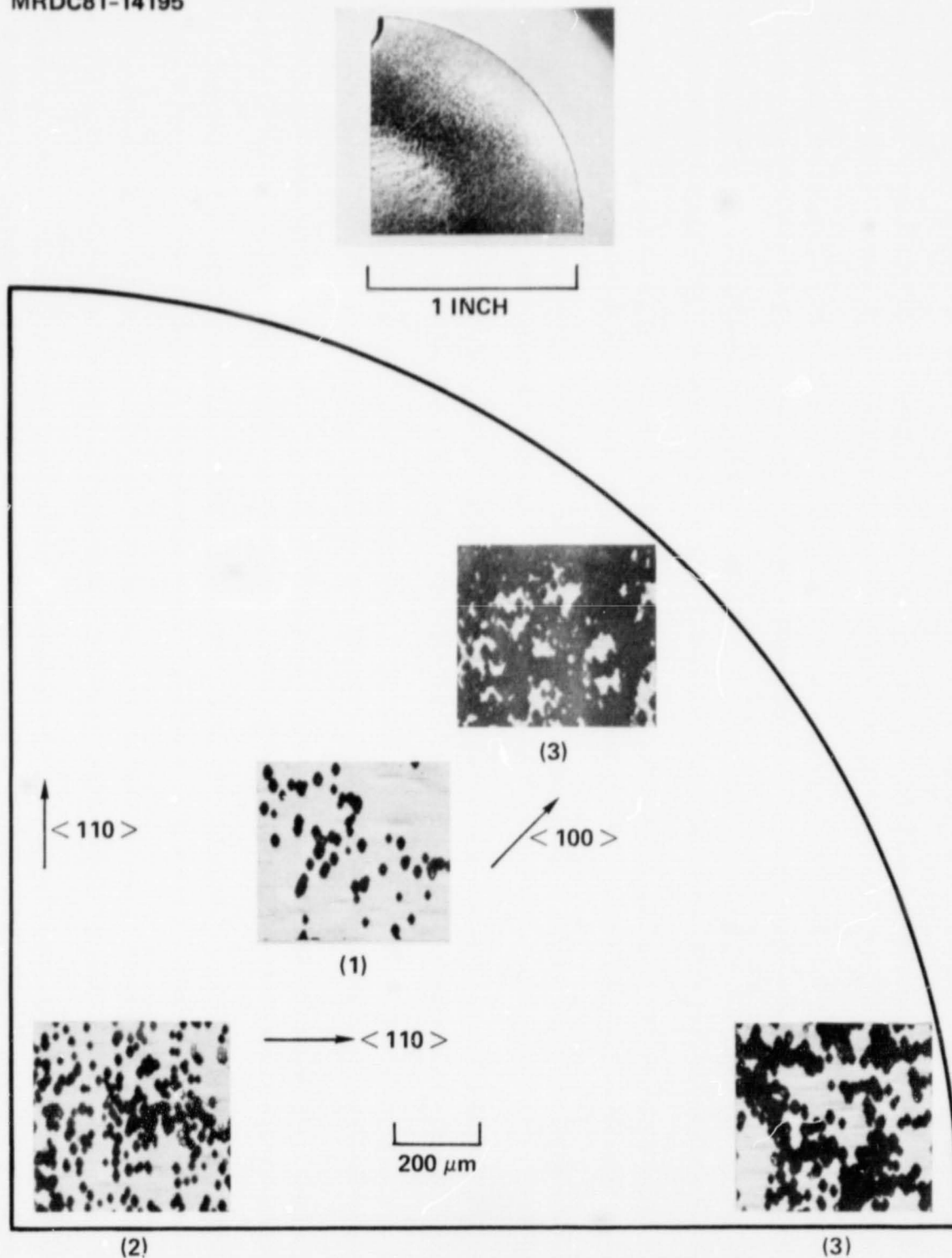


Fig. 11 Micrograph of the radial dislocation distribution for a 3-inch diameter (100) wafer from ingot R11/M.

predictions* based on a thermoelastic analysis of Czochralski growth, in which crystallographic glide induced by the excessive thermal stresses arising during the growth process is assumed to be the primary cause for the observed dislocation density patterns.

The longitudinal variation (along the growth direction) of the dislocation density and distribution was also studied by comparing the radial dislocation density of wafers cut from the front, middle, and tail of the crystal. The average dislocation density increases from the front to the tail of the crystal. This effect is probably due to both the multiplication of dislocations and to an increase in the level of thermally-induced stress in the crystal as the growth process continues.

4.2.2 Peripheral Ga Inclusions

Small (0.1 - 1 millimeter diameter) Ga droplets were observed around the edge of several wafers. The droplets apparently had penetrated the surface of the crystals to a depth of up to about 2 millimeters. The droplets formed as a result of the preferential evaporation of As from surface of the crystal during growth. The penetration was due to the thermal migration of the droplets from the cooler surface to the hotter interior. The direction of motion was probably downward rather than horizontal. We observed that significant penetration occurred only when the diameter of the crystal increased. Therefore, good diameter control precludes the penetration of Ga inclusions.

*A.S. Jordan, R. Caruso and V. R. Von Neida, Bell Systems Tech. J. 59, 593 (1980).



4.2.3 Growth Parameters Affecting the Dislocation Density

The effects of the following five growth parameters on the dislocation density were studied:

1. Dash-type seed necking
2. Seed quality control
3. Ingot cone shape control
4. Diameter control
5. Ingot diameter (2-in. vs. 3-in.)

Table VI summarizes both the variation of these growth parameters from crystal to crystal and the results of the dislocation density measurements. The EPD is shown for the "center , ring," and "edge" regions of wafers cut from the front and tail of the crystals. The results obtained from three crystals grown on the MRDC IR&D program, which were produced by with combinations of growth conditions not used on the NASA crystals, are also shown for information purposes.

To evaluate the effectiveness of the seed quality and Dash-type seed necking procedure in reducing the dislocation density, crystals grown with a high or low dislocation density seed as well as with or without a thin neck were compared. Horizontal Bridgman grown $\langle 100 \rangle$ seeds with etch pit densities varying from 1.5×10^3 to $5.0 \times 10^5 \text{ cm}^{-2}$ were used. Neck diameters as small as 1.2 millimeters with lengths of up to 20 millimeters were grown. The EPD results on the 3-in. diameter front wafers of the crystals grown with different seed quality and necking procedures are shown in Table VI. The results clearly demonstrate that for the crystals with the cone angles between



25 and 65°, a dislocation density of less than $2.5 \times 10^4 \text{ cm}^{-2}$ can be achieved in both the center and ring regions by employing low dislocation seeds with and without the necking procedure (R17, R18, R28, R38), as well as by employing high dislocation seeds in conjunction with the necking procedure (R15). It will be shown later that no empirical correlation was found between the cone angle and dislocation density for the cone angles between 25 and 65°. One can therefore conclude that the Dash-type seed necking procedure is effective for growing low dislocation density LEC GaAs only when using high dislocation density ($>10^4 \text{ cm}^{-2}$) seeds. In practical terms, this result shows that seed necking can be eliminated from the growth procedures for large-diameter LEC crystals by careful selection of high quality seeds.

In order to explain the above results, dislocation maps of longitudinal cross sections of the different crystal necks were analyzed. For neck diameters less than 2.5 millimeters, slip traces formed after growth as a result of the large stresses induced by the weight ($\sim 2.4 \text{ Kg}$) of the crystal. For neck diameters greater than 2.5 millimeters, dislocation density maps of neck regions, as shown in Fig. 12 (R16), indicate a significant reduction in dislocation density after necking. However, as soon as the crystal starts to grow out after necking, the dislocation density increases to approximately $4 \times 10^3 \text{ cm}^{-2}$, which is comparable to the dislocation density of high quality commercial seeds. This finding clearly shows that the seed necking procedure is effective for growing low dislocation density crystals only when using high dislocation seeds.



Table VI
Summary of Etch Pit Density (EPD) Measurement on LEC Ingots

| Diameter | Seed | EPD (cm ⁻²) Front | Tail | Seed Necking | Remark Cone | Diameter Control |
|--|-----------------------|---|---|--------------|----------------|---------------------|
| <u>A. Ingots grown under NASA program</u> | | | | | | |
| R 11/M ~ 3 in. | 5 x 10 ⁴ | 1 4.0 x 10 ⁴ 2 1.4 x 10 ⁵ 3 4.0 x 10 ⁵ | 1 3.5 x 10 ⁴ * 2 2.0 x 10 ⁵ * - | No | 10° | ±9.3 mm |
| R 14/C 2 in. | 2 x 10 ⁵ | 1 2.3 x 10 ⁴ 2 4.4 x 10 ⁴ 3 1.2 x 10 ⁵ | 1 6.3 x 10 ⁴ Δ 2 1.3 x 10 ⁵ Δ 3 2.2 x 10 ⁵ Δ | No | 50° | ±1.0 mm |
| R 17/M ~ 3 in. | 5.5 x 10 ³ | 1 1.8 x 10 ⁴ 2 2.6 x 10 ⁴ 3 8.0 x 10 ⁴ | 1 8.6 x 10 ⁴ 2 7.7 x 10 ⁴ 3 2.0 x 10 ⁵ | Yes | 50° | ±3.0 mm |
| R 18/M ~2 1/2 in. | 6.0 x 10 ³ | 1 1.0 x 10 ⁴ 2 2.5 x 10 ⁴ 3 5.6 x 10 ⁴ | 1 2.5 x 10 ⁴ * 2 3.9 x 10 ⁴ * 3 7.6 x 10 ⁴ * | Yes | 40° | ±8.5 mm |
| R38/M ~3in. | 1.0x10 ⁴ | 1 1.1x10 ⁴ 2 2.0x10 ⁴ 3 1.1x10 ⁵ | 1 1.5x10 ⁵ 2 2.5x10 ⁵ 3 1.7x10 ⁵ | Yes | 25° | ±1.5 mm |
| <u>B. Ingots grown under Rockwell IR&D program</u> | | | | | | |
| R 5/M ~ 3 in. | 5 x 10 ⁴ | 1 7.6 x 10 ⁴ 2 4.6 x 10 ⁴ 3 3.0 x 10 ⁵ | 1 6.1 x 10 ⁵ 2 6.1 x 10 ⁵ 3 1.1 x 10 ⁶ | No | 30° | ±10.0mm |
| R 15/M ~ 3 in. | 5 x 10 ⁵ | 1 1.5 x 10 ⁴ 2 3.0 x 10 ⁴ 3 1.7 x 10 ⁵ | 1 1.2 x 10 ⁵ 2 1.4 x 10 ⁵ 3 2.1 x 10 ⁵ | Yes | 65° | ±8.5mm |
| R 28/M ~ 3 in. | 3.5 x 10 ³ | 1 7.3 x 10 ³ 2 1.3 x 10 ⁴ 3 1.9 x 10 ⁵ | 1 8.1 x 10 ⁴ 2 9.0 x 10 ⁴ 3 3.0 x 10 ⁵ | No | 30° | ±1.5 mm |

1: Ring area between center and edge, 2: center,
3: ~ 1/5 in. wide edge area.
*: Cut from ~ 1/2 ingot length area
Δ: Cut from ~ 2/3 ingot length area
M: Manual; (100) growth, C: coracle; (111) growth.



The effect of the cone angle on the dislocation density was investigated by comparing crystals grown with cone angles from 10 to 65°. Crystals with a cone angle of 10° or less are referred to as "flat-top" crystals. Table VI summarizes our results. Crystals grown from low dislocation density seeds or from high dislocation seeds with thin necks were compared to minimize effects of variation in measured EPD due to variable seed quality. The results show that low dislocation densities can be achieved by crystals grown with 25 to 65° cones; no empirical correlation between the cone angle and dislocation density was observed for these crystals in the present study. This finding is in disagreement with previous investigations on LEC GaAs and GaP crystal growth**, which reported that the dislocation density can be substantially reduced using large cone angles (gradual cone). To resolve this discrepancy, detailed analyses of longitudinal cross-sections of crystal cones are underway to chart the propagation of dislocations as the crystals grew out from the neck to full diameter. The results will be presented and discussed in the final report of the follow-on program of the present project. Finally, the "flat-top" crystal (R11) showed unusually high dislocation densities. These high densities were probably induced by the severe thermal shock encountered as the crystal emerged from the B₂O₃. Therefore it can be concluded that low dislocation densities can be achieved independent of the cone angle provided that the crystal is not flat-topped. In practical terms, the achievement of low dislocation growth with shallow cones will provide tremendous savings in growth time and materials.

**P.J. Roksnoer, J.M.P.L. Huijprechts, W.M. Van De Wiggert and A.J.R. De Kock, J. Crystal Growth 40, 6(1977).

MRDC81-12824

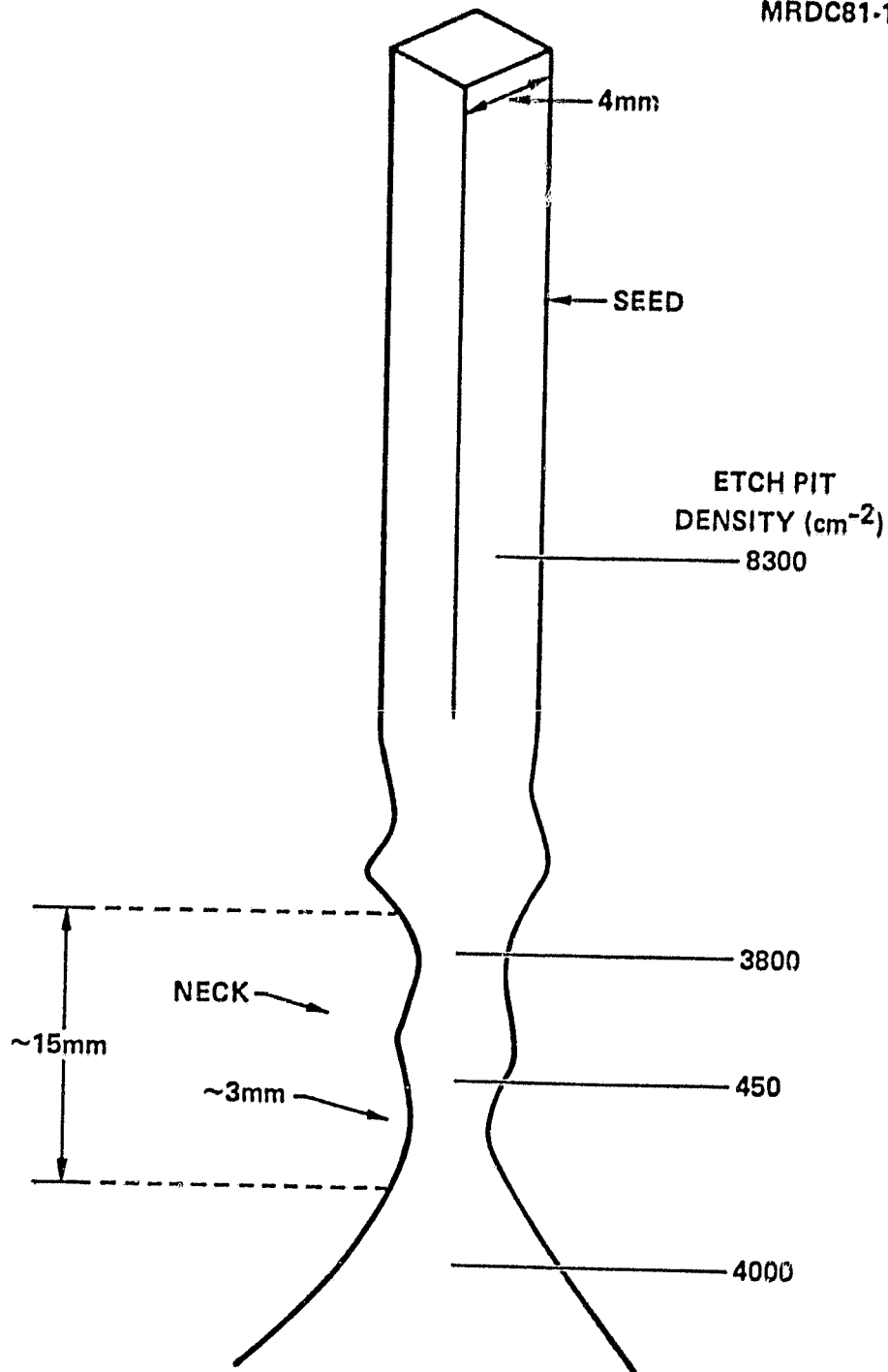


Fig. 12 Schematic of seed, neck, and top of cone showing variation in etch pit density due to seed necking (R16).

Regarding the effect of absolute diameter on the dislocation density, a sufficient number of 2-in diameter crystals have not yet been grown to make valid comparison with 3-in crystals. The dislocation density could be expected to decrease as the diameter decreases as a result of reduced radial temperature gradients in the crystal during growth. However, no dramatic effects were observed in smaller diameter crystals. For example R14 was grown with the coracle and has excellent diameter control. However, the seed was of poor quality and no neck was grown. The relatively high dislocation density is therefore attributed to poor seed quality. R18 exhibited good crystalline quality in the front of the ingot, but not as good as some of the 3 in. - diameter crystals. Again, some other parameter, such as the seed quality, probably played a more important role. Further work is needed in this area.

Finally, the effect of diameter control (deviation of diameter from the mean) was evaluated by comparing the dislocation densities of the tails of the crystals. For example, R15, R17, R28 and R38, were all grown from low-dislocation-density seeds or high-dislocation-density seeds with thin necks. The major differences in growth parameters lay in the cone angle and diameter control. From examination of the results, it can be concluded that the cone angle had little effect on the formation of dislocations in these crystals. However, there is general a correlation between reduced dislocation densities and reduced diameter deviations. These results suggest that, although zero diameter deviation is prescribed for maximum effect, good results can be obtained under practical crystal growth conditions by maintaining the diameter to within ± 3 millimeters.

5.0 SUMMARY

Two important milestones have been achieved on the NASA "Preparation of High Purity Low Dislocation Density GaAs Single Crystals" program. First, it has been shown that the concentration of background impurities in LEC material can be reduced to the level of $4 \times 10^{15} \text{ cm}^{-3}$ through proper control of the materials synthesis and growth conditions. This degree of purity is comparable, if not superior to that of commercial Bridgman material. It is achieved by using high purity starting materials and crucibles, by using the in-situ synthesis technique, and by controlling the amount of moisture in the boric oxide encapsulant.

Second, it was shown that the average dislocation density throughout the entire central region (defined by about 85% of the diameter) of 3-inch substrates can be controlled to a value below about $2 \times 10^4 \text{ cm}^{-2}$. The dislocation density in selected regions can be as low as 3000 cm^{-2} (observed at 2.5 in diameter). These results represent a substantial improvement over commercial LEC material, which typically has a dislocation density on the order of 10^5 cm^{-2} at 2-inch diameter. Important parameters in the control of the dislocation density are diameter control, and seed quality in conjunction with the use of Dash-type necking. Furthermore, the dislocation density is independent of the cone angle provided that the crystal is not flat-topped. Finally, no effect of absolute diameter has been observed for diameters greater than 2 inches.

The capability of producing bulk GaAs with a low background impurity concentration has significance for solar cell applications requiring doped

wafers depending on the function of the substrate in the device. In devices where the substrate is passive, such as in the conventional "buffered" GaAs-GaAlAs heterostructure cell, out-diffusion from the substrate to active regions of the device of fast-moving metallic impurities such as Fe must be minimized. These impurities act as carrier traps, reducing the minority carrier lifetime, and as compensation centers, changing the effective carrier concentration of the region in which diffusion takes place. These factors combine to reduce overall cell performance and radiation hardness. Lower levels of background impurities will result in fewer impurities reaching the active region of the device. Thus, adverse effects from out-diffusion are expected to be minimal with LEC GaAs.

For solar cell structures where the substrate plays an active role in the device, low background contamination will lead to low electrical compensation provided that the doping level of donors (acceptors) is about a factor of 5 or more greater than the background concentration of acceptors (donors). Low compensation in turn results in high carrier mobility and a high minority carrier diffusion length. On the basis of impurity analysis in this program, good electrical characteristics can be expected in n- and p-type LEC material doped at about $5 \times 10^{16} \text{ cm}^{-3}$ and higher. This doping level is at least one order of magnitude lower than that of substrate material in conventional (passive) solar cell structures, and similar or lower in magnitude to doping levels in devices with active substrates. Therefore, LEC material will be applicable to most solar cell applications on the basis of purity and electrical properties.

Intentionally doped n- and p- type LEC GaAs with low compensation and high minority carrier diffusion lengths can be grown from both quartz and PBN crucibles. However, semiconductor-quality p-type material must have a low background concentration of Si. Therefore "wet" boric oxide must be used for the growth of p-type material from quartz crucibles. PBN can be used for both n- and p-type material.

As a result of MRDC's progress attained during the NASA program in understanding the cause-effect relationships between the dislocation density and crystal growth conditions, 3-inch diameter crystals were recently grown with an average dislocation density in the "ring" region of 7500 cm^{-2} . The dislocation densities throughout the entire central region of the substrate (defined by 85% of the crystal diameter) in the front of the crystal was less than $2 \times 10^4 \text{ cm}^{-2}$. These densities are the lowest reported in any LEC material of comparable diameter. Just as striking is the fact that the dislocation density in the "center" and "ring" region of substrates obtained from the tail of the crystals are lower than $1 \times 10^5 \text{ cm}^{-2}$, which is less than the density observed in substrates obtained from the front of 2-inch-diameter commercial LEC crystals.

The capability of producing 3-inch-diameter GaAs ingots with dislocation densities in the 10^4 cm^{-2} range from front to tail is extremely important for solar cell applications where radiation hardness as well as efficiency is critical. This is because the minority carrier diffusion length is not significantly effected by the presence of dislocations until the spacing between dislocations is comparable to the diffusion length. The inter-dislocation spacing in MRDC 3-inch ingots now ranges from about 32 to



115 microns at the tail and front of the ingots, respectively. This distance is substantially longer than the minority carrier diffusion length in n and p-type material of 1-2 and 5-20 microns, respectively. Therefore, doped LEC material with dislocation densities in the 10^4 cm^{-2} range is expected to exhibit good minority carrier diffusion lengths.

This investigation into crystal growth methods for minimizing the dislocation density of LEC GaAs will ultimately impact the cost-effectiveness of the LEC techniques. For example, it has been shown that cone-growth can be virtually eliminated from the crystal growth while preserving the structural quality of the crystal. This capability will increase the yield of full diameter wafers per crystal, and substantially reduce the time required to grow each crystal. Both factors will lead to cost reductions to the user.

Finally, it is important to note that the dislocation density of intentionally doped GaAs is generally lower than in undoped material under the appropriate crystal growth conditions. The mechanism is not yet well understood. Although the concentration of impurities in the crystals grown to date has not been sufficiently high to exert this effect, lower dislocation densities are anticipated in more heavily doped material to be grown in the near future. This work, which is being conducted exclusively at MRDC, should prove to be critical to the development of a large-area solar cell production capability.